AIMdyn, Inc.
Engineering Consulting & Software Development

Distribution Statement A. Approved for public release. Distribution is unlimited.

Contract: **N00014-18-P-2004** **Date: 09/30/2018**
Project Title: Analysis and Prediction of Sea Ice Evolution using Koopman Mode Decomposition Techniques
Subject: Monthly Progress Report
Period of Performance: August 31, 2018 – September 30, 2018

To: Program Officer: Office of Naval Research
Dr. Reza Malek-Madani ONR Code 31
875 N. Randolph St.
Arlington, VA 22203-1995
E-mail: reza.malekmadani@navy.mil

Office of Naval Research
Ana Lugaro
875 N. Randolph Street
Arlington, VA 22203-1995
E-Mail: ana.lugaro1@navy.mil

ACO: Shellyn Conklin
DCMA Los Angeles
E-mail: shellyn.conklin@dcma.mil

Director, Naval Research Lab Attn: Code 5596
4555 Overlook Avenue, SW
Washington, D.C. 20375-5320
E-mail: reports@library.nrl.navy.mil

Defense Technical Information Center
8725 John J. Kingman Road STE 0944
Ft. Belvoir, VA 22060-6218
E-mail: tr@dtic.mil; dtic.belvoir.ecm.mbx.tr@mail.mil

AIMdyn, Inc. respectfully submits Progress Report 6 for contract N00014-18-P-2004**.** Please direct any Technical questions on this report to the undersigned.
V/r

Dr. Maria Fonoberova
1919 State Street, Suite 207
Santa Barbara, CA 93101
mfonoberova@aimdyn.com

Business Status Report

(1) Resource Status:
Resourced to plan.

(2) Contributions by AIMdyn Inc:
See technical report.

(3) Resource status VS Original schedule:
On plan to original scope of work. Effort is fixed priced.

PROGRAM FINANCIAL STATUS

Work Breakdown	Cumulative to Date	At Completion
CLIN#0001-CLIN#0006	$112,125	$112,125

Structure or Task Element	Planned Expend	Actual Expend	% Budget Compl	At Compl	Latest Revised Estimate	Remark Remark
CLIN#0006	$18,690	$18,690	100%	100 %	N/A	N/A

Subtotal: $18,690
Management Reserve: N/A
Or Unallocated Resources: N/A
TOTAL: $18,690

Technical Status Report

Abstract

The prediction of future sea ice concentration in the northern and southern hemisphere was performed using Koopman Mode Decomposition for varied year ranges and prediction years. For prediction one year in the future, it was found that northern hemisphere sea ice concentration was better predicted with longer year ranges as inputs to Koopman Mode Decomposition, and the prediction success varied differently for different years and year ranges in different regions.

ACCOMPLISHMENTS

Summary

The Koopman Mode Decomposition (KMD) based prediction procedure was applied to all of the sea ice concentration data for both hemispheres as a whole and for defined regions within each hemisphere, for KMD input year windows between 3 and 38 years and for prediction years between 1982 and 2017. The goodness of the prediction results for one year in the future was generally better for the northern hemisphere than the southern hemisphere, and specific regions showed better results for different input year windows and at different prediction years, suggesting different dynamics between different regions.

Introduction

Previous reports presented prediction results for selected input year windows (i.e. the years used as input to the KMD algorithm) and prediction years. Presentation of prediction results for a wide range of year windows and prediction years is desirable but presents a challenge in data visualization due to the dimensionality of the data (that is, there are prediction results for years between 1982 and 2017, where multiple predictions are made for each year from the different year window ranges from different numbers of years prior to the prediction year, and the character of the prediction can change with the season in each year). To produce the most useful and easily interpreted data visualization, it was decided to reduce the dimensionality of the results by only considering predictions one year in the future (e.g., for an input year range of 1979-1981, only the prediction for 1982 is shown), and instead of presenting results for all twelve months of the year in one figure, separate figures are shown for the two months of greatest interest: the month where the sea ice concentration is at a maximum (March in the northern hemisphere and September is in the southern hemisphere) and the month where the sea ice concentration is at a minimum (September in the northern hemisphere and February in the southern hemisphere). Examination of these extrema months can give a better sense of the usefulness of KMD techniques for predicting trends in the sea ice dynamics.

Also, the geographic division of the southern hemisphere was redone to include a greater number of coastal regions and the ocean area associated with those coastal regions. These

regions match those commonly used for the Antarctic by researchers, with the exception that traditionally the Amundsen and Bellingshausen Seas are combined into one region but here we split them into separate regions to expose any potential differences in their behavior.

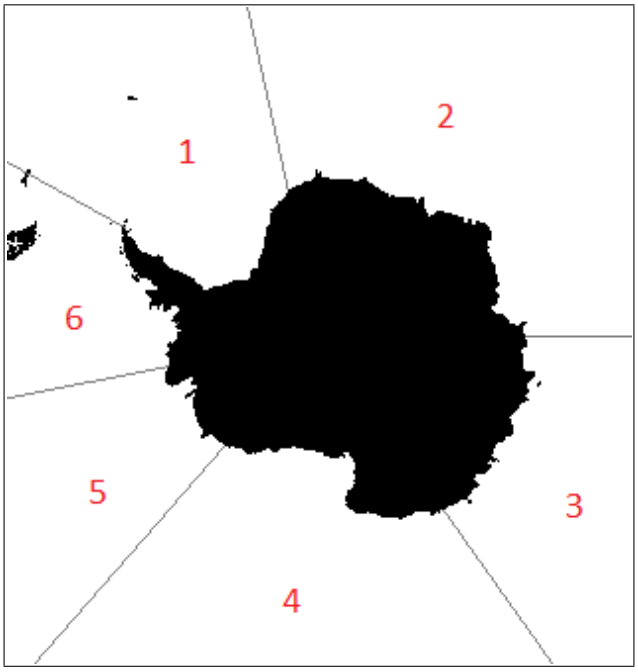

Figure 1: Southern hemisphere geographic regions considered in reconstruction results shown here. 1: Weddell Sea, 2: Indian Ocean, 3: West Pacific Ocean, 4: Ross Sea, 5: Amundsen Sea, 6: Bellingshausen Sea.

Methods

As described in the previous report, reconstruction of the N_p sea ice concentration pixel values $\mathbf{C}$ at discrete time step k is performed using the Koopman eigenvalues λ_j and the Koopman modes $\mathbf{v}_j$ obtained from applying KMD to the concentration values over N time steps (months, in this case):

$$\mathbf{C}_k = \sum_{j=1}^{N} \lambda_j^{k-1} \mathbf{v}_j$$

Here, there are N Koopman eigenvalues and Koopman modes, where each Koopman eigenvalue is a single complex number and each Koopman mode has dimensions 1 by N_p.

For $1 \leq k \leq N$, $\mathbf{C_k}$ is termed a reconstruction of the kth time step in the original data $\mathbf{C}$, as the Koopman eigenvalues and modes came from a decomposition of the observations over this time range and should simply reproduce the data used as input to the KMD. For $k > N$, $\mathbf{C_k}$ is a prediction of the future behavior of the sea ice concentration for the (future) kth time step, based on the system dynamics deduced from decomposition of earlier observations.

KMD reconstruction was performed on all data from the given hemisphere, then the pixels corresponding to each region were identified and compared with actual data (when

available). Note that an alternate approach, not shown here, is to apply KMD to only the data from a particular region and then perform reconstruction for that region using those KMD results. It was found that the predictions produced using only the data from a particular region were less accurate than predictions from applying KMD to the entire hemisphere of data, presumably due to the lower dimensionality of the former case.

As before, two methods were applied to visualize the "goodness" of the KMD reconstruction results. The first was based on a direct pixel-to-pixel comparison of the actual data and prediction results. In this case, the calculation consisted of, for each month and for each region, taking the mean of the absolute value of the difference between the actual data and prediction results for all pixel values for which either the actual data or prediction results contained a sea ice concentration value greater than zero. The reason for restricting consideration to nonzero concentration pixels was to avoid giving a misleading impression of the goodness of the prediction results, particularly when there is a large fraction of ice-free pixels in lower latitude regions and in the summer. The second visualization method was to plot the mean sea ice concentration value of the actual data and prediction results in each region. This approach does not judge the exact geographic precision of the prediction results but provides a broader sense of whether the predictions match the actual increase or decrease of sea ice in a particular region.

Results and Discussion

Figure 2 shows the actual mean sea ice concentrations for the 39 year period of data for the newly defined southern hemisphere regions described previously. Dividing the hemisphere into six regions instead of the four considered shows the longitudinal variations in regional dynamics in greater detail. Also note that while the Amundsen and Bellingshausen Seas show temporal variation of a similar character, their multi-year variations are not obviously correlated, which motivated our decision to consider them as separate regions.

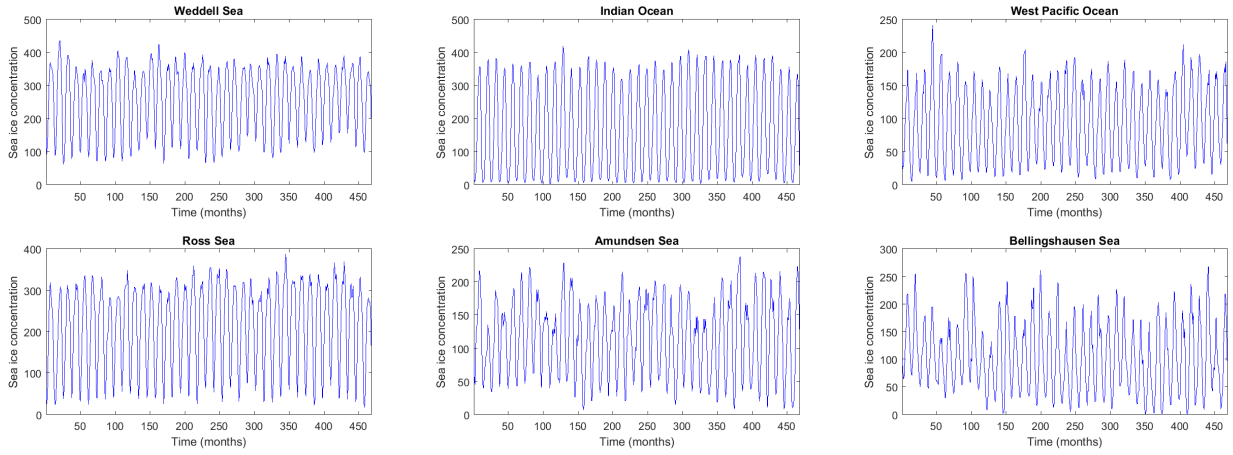

Figure 2: Time series of monthly average sea ice concentration (1000=100%) for southern hemisphere regions.

The goodness measures of the prediction for the newly defined southern hemisphere regions are shown in Figures 3 and 4. Figure 3 shows the results for the first method

of judging the goodness of the prediction (the mean of the absolute difference between the actual and predicted results), for the southern hemisphere for predictions for 2014-2017 using the previous 30 years of data. The error is similar for each region, and shows an apparent slow increase over time.

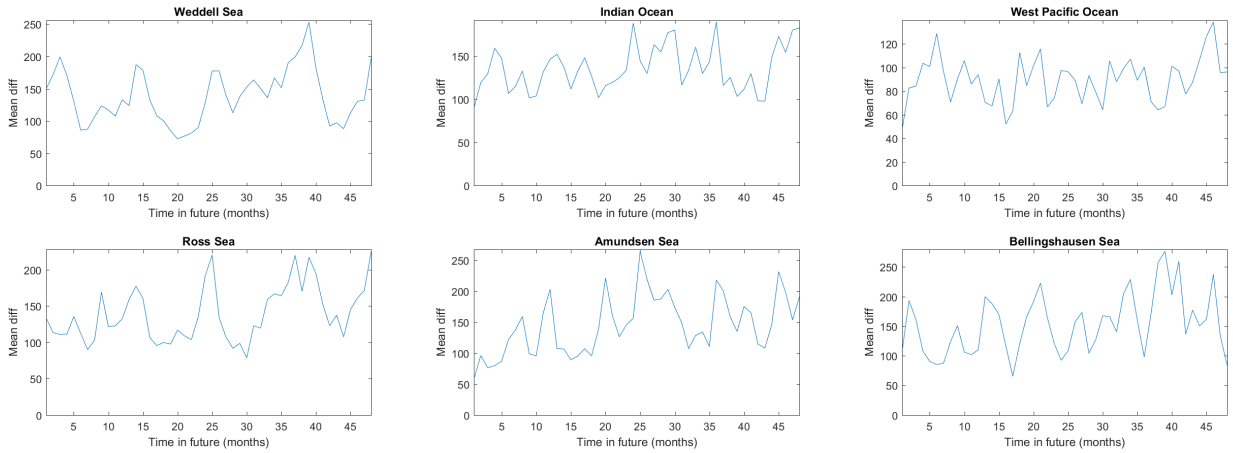

Figure 3: Goodness of southern hemisphere prediction results, based on summing the absolute value of the difference between the actual data and prediction results for all pixel values for which either the actual data or prediction results contained a sea ice concentration value greater than zero. Prediction is based on KMD of 30 year data range (1984 to 2013) and prediction of four future years. Vertical axis units are sea ice concentration (1000=100%).

Figure 4 shows the mean of the actual data (blue lines) and predictions (red lines) for each region, showing the general trends of sea ice concentration in each region. It is seen that in the first year, the prediction of the maximum sea ice concentration is very good for each region, and even the minimum for the following year is well predicted in the Weddell Sea, West Pacific, and Amundsen Sea.

Figures 5 to 12 are 2-D representations of the goodness of the prediction for the next year, for the single months of the year with the minimum and maximum sea ice extent for varied KMD window widths. The goodness measure is the error of the prediction result, specifically the difference between the prediction result and the actual sea ice concentration for a particular month (recall that here concentration is shown in tenths of a percent, i.e. 1000 corresponds to 100% concentration). The horizontal axis of the figure is the year of the month predicted, and the vertical axis is the number of years used as the input to the Koopman mode decomposition used to perform future prediction. Note that for each prediction year, the year range used for KMD prediction immediately precedes the prediction year, e.g. for prediction year 2017, a 3 year window width consists of the years 2014-2016, a 10 year window width consists of the years 2007-2016, and so on. Because the sea ice concentration data used is only available starting from the year 1979, the maximum possible window width increases by one year per year after 1979, up to a maximum window width of 38 years for predictions of the year 2017. The minimum window width was chosen to be 3 years, so the figures show prediction years between 1982 and 2017 and window widths between 3 and 38 years.

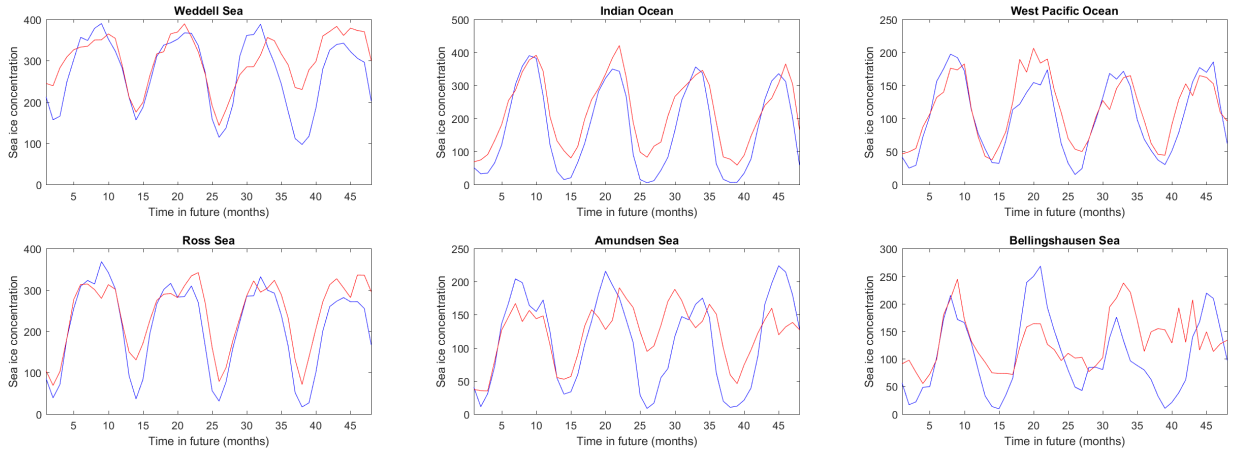

Figure 4: Comparison of actual (blue) and predicted (red) southern hemisphere mean sea ice concentration. Prediction is based on KMD of 30 year data range (1984 to 2013) and prediction of four future years. Vertical axis units are sea ice concentration (1000=100%).

The color scale of the figures highlights the deviation from zero of the prediction error, where red and blue show when the prediction is greater than or less than the actual data, respectively, and darker colors indicate larger magnitude errors (note that the color maps are not symmetric about zero, however). Points that are colored white indicate that the prediction was in good agreement with the actual data, therefore regions of white or light colors indicate combinations of window widths and prediction years that were found to successfully predict future sea ice annual minimum and maximum concentrations. Large regions of white/light colors are of more interest than isolated pixels, because robust prediction capabilities are desired, and isolated prediction successes could be attributed to random chance rather than legitimate predictive ability.

Figure 5 shows the prediction error for March (when the sea ice annual concentration maximum occurs) for the entire region of the northern hemisphere covered by the available satellite data. For most years, the best prediction results occur for windows of at least 10 years and the goodness generally improves with window width. Years where the prediction goodness is relatively poor and does not significantly improve with increasing window width are generally years with a large change from one year to the next.

Figure 6 shows the prediction error for September for the entire covered region of the northern hemisphere, when the sea ice annual minimum occurs. In contrast to the results for the sea ice maximum, the prediction error is not generally better for longer windows.

Figures 7 and 8 show northern hemisphere prediction results for March and September for specific geographic regions. Generally, longer windows are seen to produce better prediction results, but there is significant variation between different regions and no single window width range is obviously best for all cases. This difference is presumably due to the different time scales and degree of influence of the different effects driving the dynamics of different regions.

Figures 9 to 12 show the equivalent set of figures for the southern hemisphere, where September is the month with the maximum sea ice concentration and February (not March)

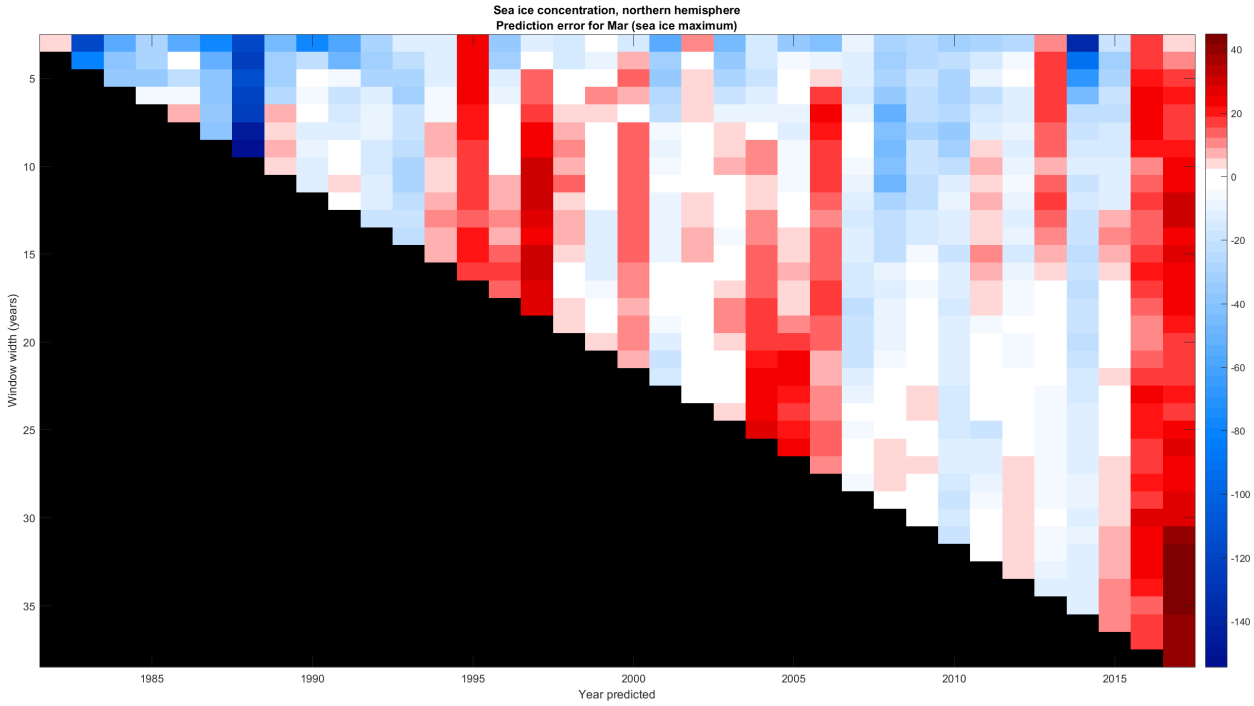

Figure 5: Sea ice concentration prediction error for the entire northern hemisphere region covered by the available satellite data, for the month of March, when the maximum sea ice concentration occurs. The best prediction results generally occur for longer time windows.

is the month with the minimum sea ice concentration. The same general comments apply to the southern hemisphere results as to northern hemisphere results, with the important difference that longer windows are generally of less benefit in the southern hemisphere case.

Conclusions

Consideration of a wide range of input year ranges and prediction years showed that KMD is generally successful at predicting sea ice concentration one or more years in the future, with generally greater success in the northern hemisphere and for certain specific geographic regions.

The observation of windows over which prediction works better are of interest, since regions where shorter time prediction works better might indicate those that are experiencing more rapid change. In addition, given the success of the current, purely data-driven methodology, adding a physical model and using the current methodology for data assimilation is an interesting prospect.

Personnel Supported

Dr. Maria Fonoberova, Dr. Igor Mezic, Dr. James Hogg

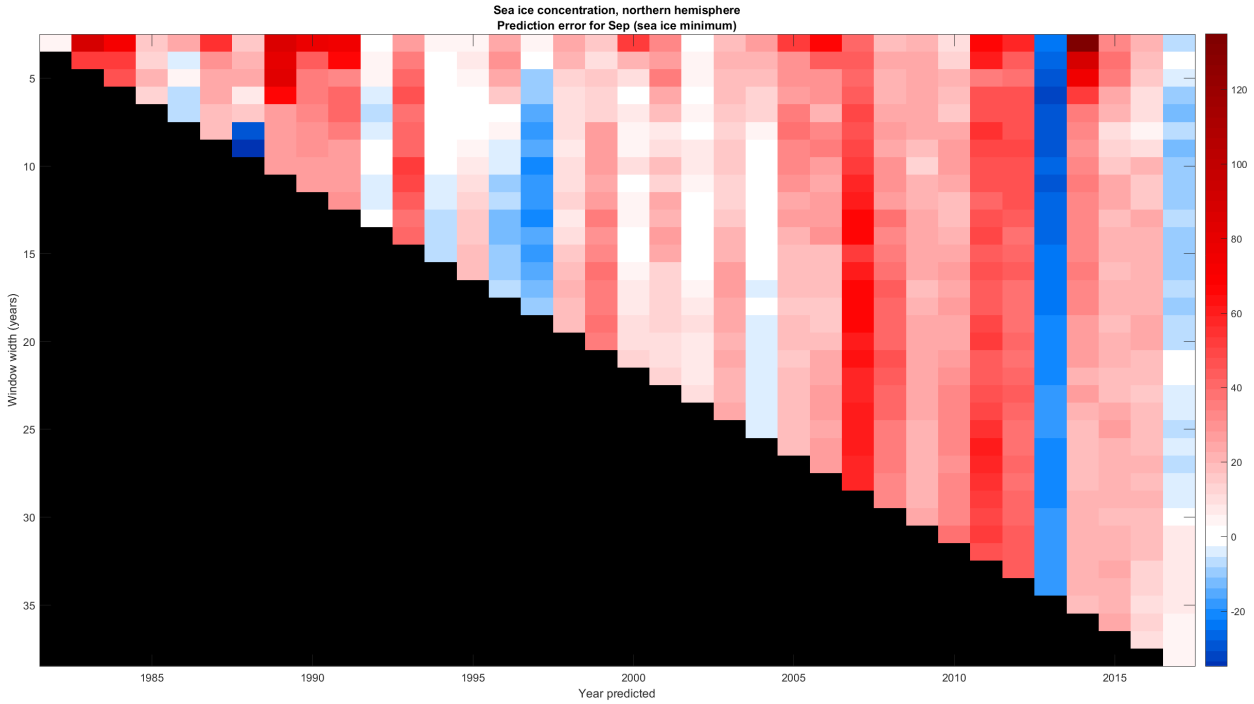

Figure 6: Sea ice concentration prediction error for the entire northern hemisphere region covered by the available satellite data, for the month of September, when the minimum sea ice concentration occurs. Here, longer windows do not as often produce better prediction results.

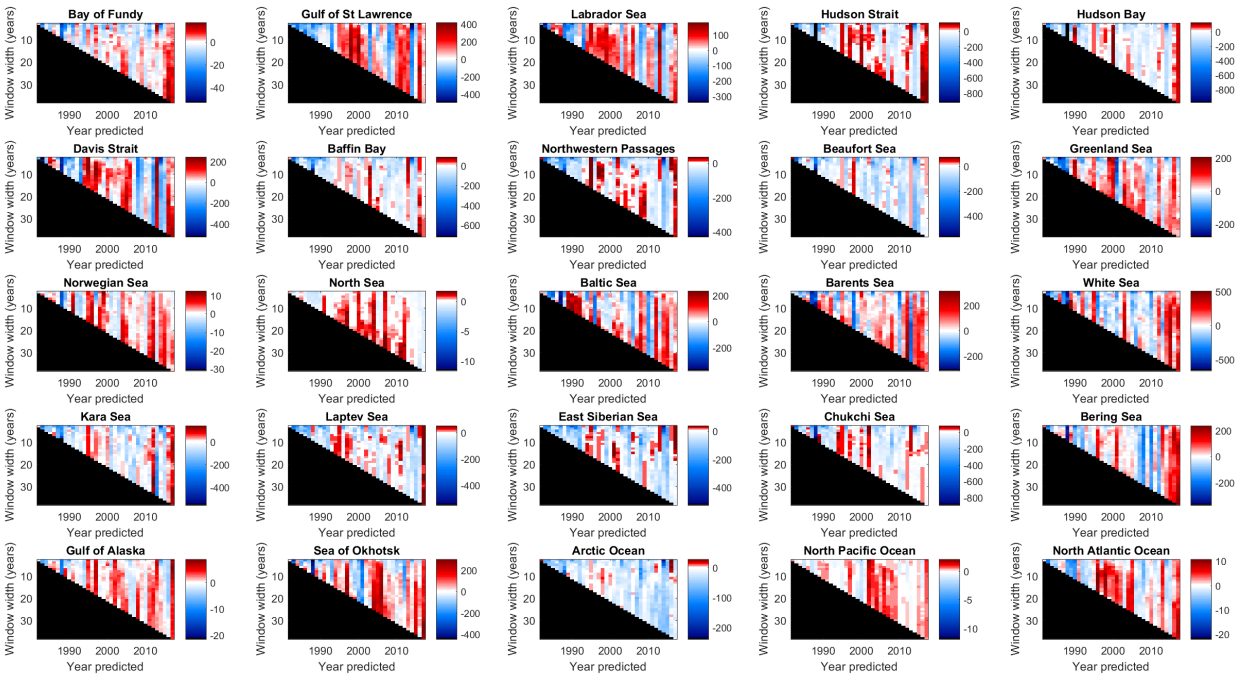

Figure 7: Sea ice concentration prediction error for the northern hemisphere regions for the month of March, when the maximum sea ice concentration occurs. Greater window widths generally produce better predictions, but the specifics vary between regions.

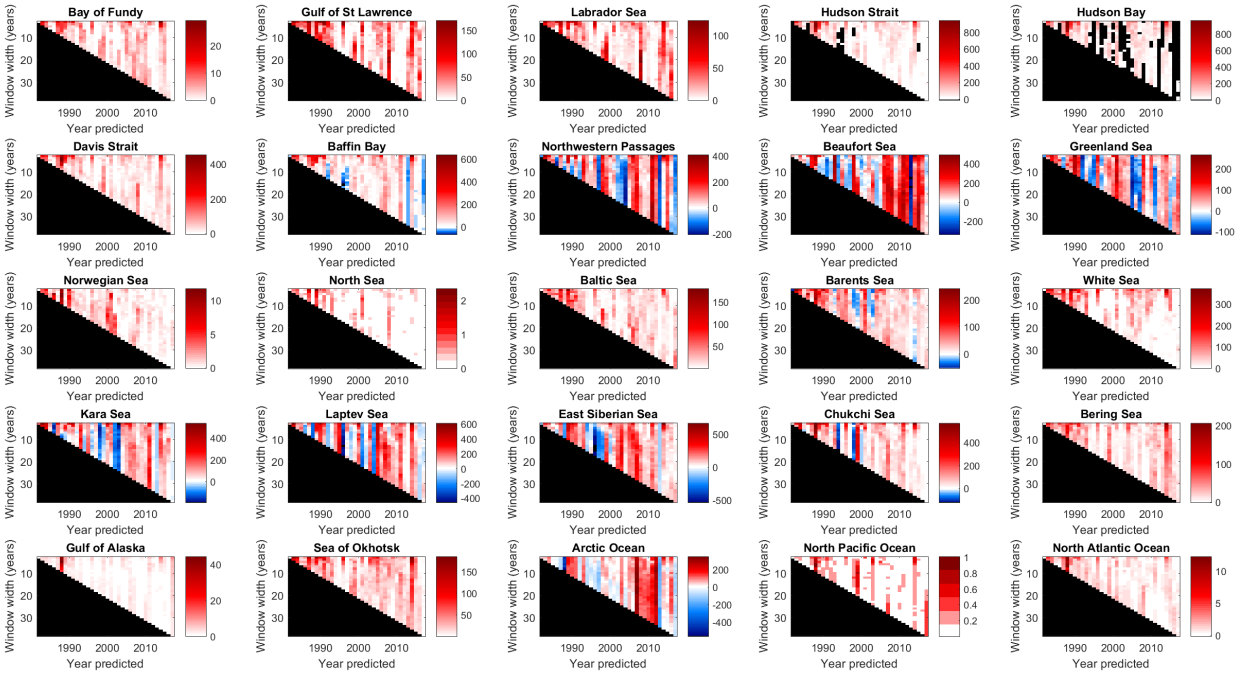

Figure 8: Sea ice concentration prediction error for the northern hemisphere regions for the month of September, when the minimum sea ice concentration occurs. As for the March case, greater window widths generally produce better predictions, but the specifics vary between regions.

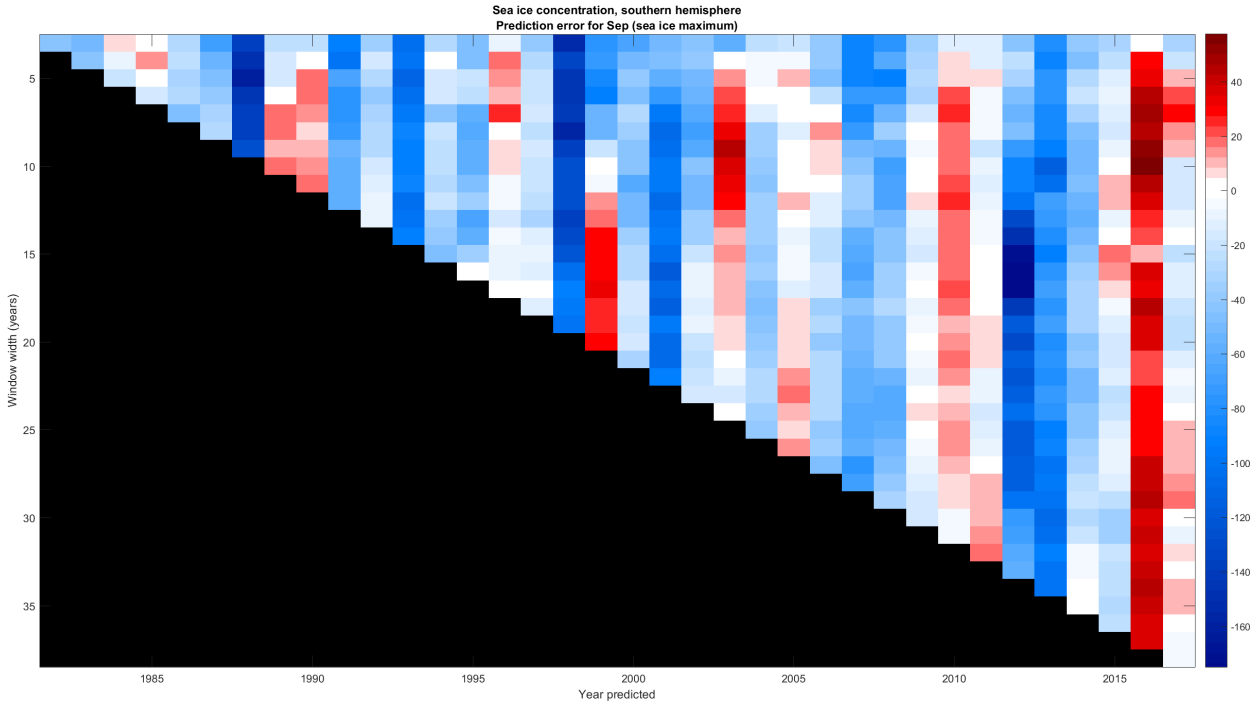

Figure 9: Sea ice concentration prediction error for the entire southern hemisphere region covered by the available satellite data, for the month of September, when the maximum sea ice concentration occurs.

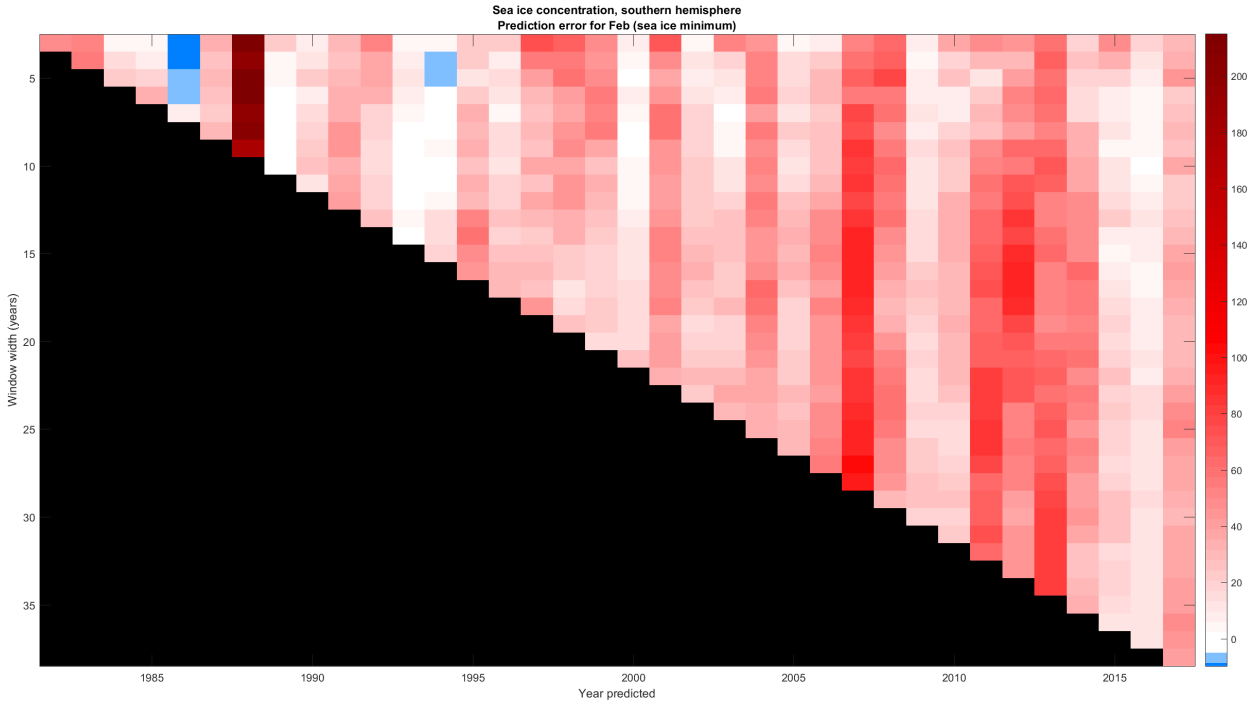

Figure 10: Sea ice concentration prediction error for the entire southern hemisphere region covered by the available satellite data, for the month of February, when the minimum sea ice concentration occurs. Here, longer windows do not as often produce better prediction results.

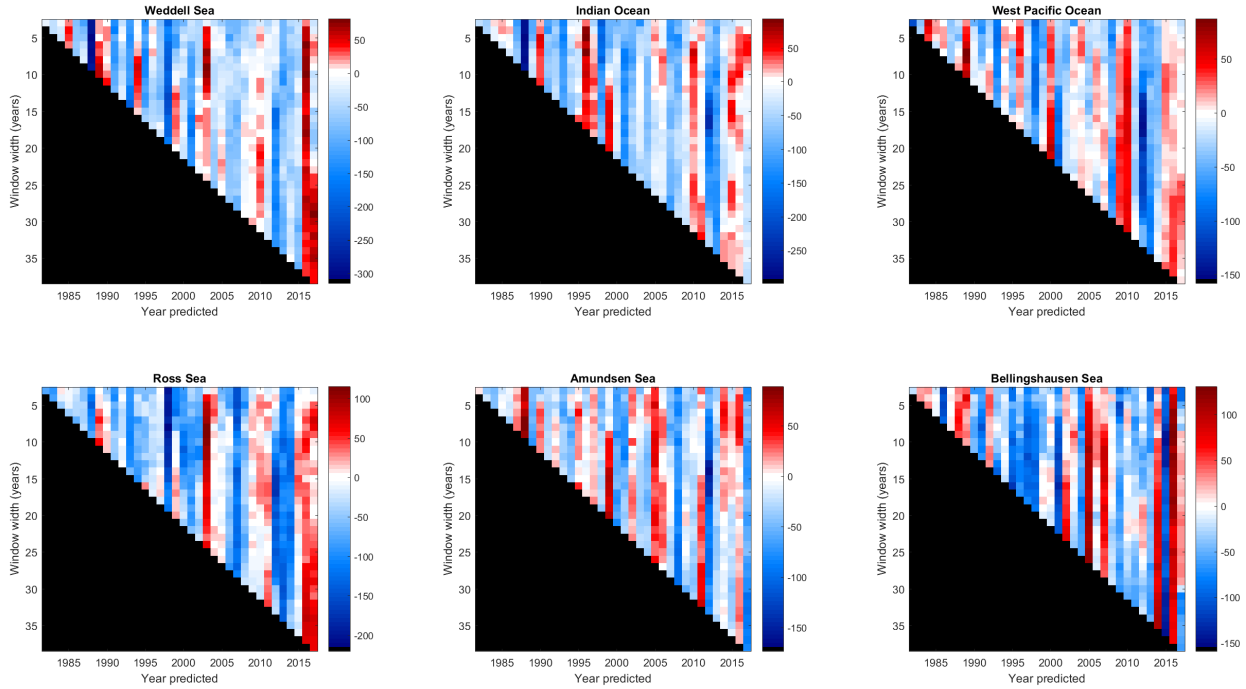

Figure 11: Sea ice concentration prediction error for the southern hemisphere regions for the month of September, when the maximum sea ice concentration occurs.

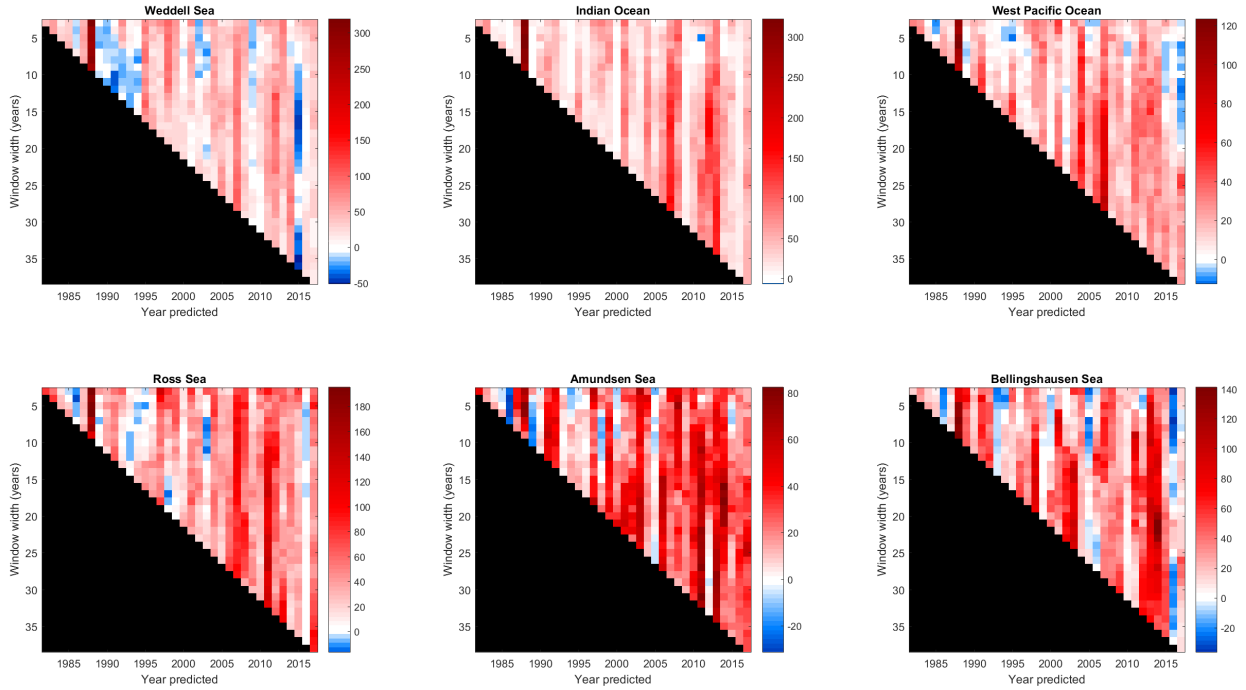

Figure 12: Sea ice concentration prediction error for the southern hemisphere regions for the month of February, when the maximum sea ice concentration occurs.